Journal of Hazardous Materials 190 (2011) 168–176

Contents lists available at ScienceDirect

Journal of Hazardous Materials

journal homepage: www.elsevier.com/locate/jhazmat

Comparison of four advanced oxidation processes for the removal of naphthenic acids from model oil sands process water

Xiaoming Liang[1], Xingdong Zhu[2], Elizabeth C. Butler*

School of Civil Engineering and Environmental Science, University of Oklahoma, Norman, OK, 73019, United States

ARTICLE INFO

Article history:
Received 23 October 2010
Received in revised form 8 March 2011
Accepted 8 March 2011
Available online 15 March 2011

Keywords:
Naphthenic acids
Oil sands
Advanced oxidation processes

ABSTRACT

Four advanced oxidation processes (UV/TiO_2, UV/IO_4^-, UV/$S_2O_8^{2-}$, and UV/H_2O_2) were tested for their ability to mineralize naphthenic acids to inorganic carbon in a model oil sands process water containing high dissolved and suspended solids at pH values ranging from 8 to 12. A medium pressure mercury (Hg) lamp was used, and a Quartz immersion well surrounded the lamp. The treatment goal of 5 mg/L naphthenic acids (3.4 mg/L total organic carbon (TOC)) was achieved under four conditions: UV/$S_2O_8^{2-}$ (20 mM) at pH 8 and 10, and UV/H_2O_2 (50 mM) at pH 8 (all with the Quartz immersion well). Values of electrical energy required to meet the treatment goal were about equal for UV/$S_2O_8^{2-}$ (20 mM) and UV/H_2O_2 (50 mM) at pH 8, but three to four times larger for treatment by UV/$S_2O_8^{2-}$ (20 mM) at pH 10. The treatment goal was also achieved using UV/$S_2O_8^{2-}$ (20 mM) at pH 10 when using a Vycor filter that transmits light primarily in the mid and near UV, suggesting that that treatment of naphthenic acids by UV/$S_2O_8^{2-}$ using low pressure Hg lamps may be feasible.

1. Introduction

Mining and extraction of bitumen for petroleum production is a growing industry [1]. Separation of bitumen from oil sands involves generation of highly alkaline process water that contains dissolved naphthenic acids at concentrations between 40 and 120 mg/L [2]. Naphthenic acids are a complex mixture of alkyl-substituted acyclic and cycloaliphatic carboxylic acids with the general chemical formula $C_nH_{2n-z}O_2$, where n is the carbon number and z is the number of hydrogen atoms lost during ring formation [3]. The pK_a of an average molecular weight component of a naphthenic acids mixture isolated by distillation was 4.5 [4], suggesting that naphthenic acids are negatively charged at neutral and alkaline pH values. Naphthenic acids are acutely toxic to aquatic biota [5].

Oil sands process water also contains total dissolved solids at concentrations of 2000–2500 mg/L, including sodium (500–700 mg/L) and chloride (75–550 mg/L) [1]. Because oil sands are a mixture of silica, clays, water, and bitumen [6], process water generated from high temperature alkaline extraction may also contain significant dissolved and suspended silica and clays. One sample of untreated tailings water from oil sands extraction contained 1000 mg/L suspended solids [7], part of which likely consisted of fine clay and silica particles. Another sample of process water from the South Texas tar sands region contained more than 400 mg/L dissolved SiO_2 [8].

Since 3 L of water are required to produce 1 L of oil from bitumen [5], treatment and recycling of process water is necessary for sustainable operation of bitumen recovery in the oil sands industry. No federal water quality criteria currently exist for naphthenic acids, but treatment to background levels of 1–5 mg/L has been recommended [1]. Allen [5] recently reviewed established and emerging treatment options for naphthenic acids and related contaminants in oil sands process water. A study of naphthenic acids degradation by ozone reported that more than 95% naphthenic acids were removed at pH 8–8.2, but without a corresponding decrease in total organic carbon (TOC), suggesting incomplete naphthenic acids oxidation under these conditions [9]. Other AOPs that rely on reactive radical species, especially hydroxyl radical ($HO^\bullet$), may be more promising for complete naphthenic acids oxidation than simple ozonation, since the hydroxyl radical is a rapid and indiscriminate oxidant [10], and treatment by ozone involves hydroxyl radicals only at elevated pH. The efficiency of radical based AOPs, however, could be compromised by the presence of anions such as carbonate and chloride that could compete for radicals, or, in a heterogeneous system, for adsorption sites on the catalyst surface [e.g., 11]. The performance of UV-based AOPs could also be hindered by suspended particles that have the potential to attenuate UV light [12].

The objective of this study was to compare four AOPs for treatment of model oil sands process waters containing naph-

* Corresponding author. Tel.: +1 405 3253606; fax: +1 405 3254217.
E-mail address: ecbutler@ou.edu (E.C. Butler).
[1] Present address: Department of Geology, University of Toronto, Toronto, Ontario, Canada.
[2] Dr. Xingdong Zhu passed away before this project was completed. This paper is dedicated to her memory.

0304-3894/$ – see front matter © 2011 Elsevier B.V. All rights reserved.
doi:10.1016/j.jhazmat.2011.03.022

thenic acids, dissolved chloride, and dissolved and colloidal silica, all at realistic concentrations. The AOPs studied were UV-illuminated TiO_2 (UV/TiO_2), UV-illuminated periodate (UV/IO_4^-), UV-illuminated persulfate (UV/$S_2O_8^{2-}$), and UV illuminated H_2O_2 (UV/H_2O_2). UV/TiO_2 and UV/H_2O_2 are commercialized technologies described in textbooks [e.g., 13]. UV/IO_4^- [14] and UV/$S_2O_8^{2-}$ [15] are promising emerging technologies. The chemistry of periodate is complex; for the range of pH values used in these experiments (pH 8–12), the predominant periodate species include IO_4^-, $H_3IO_6^{2-}$, $H_2IO_6^{3-}$, and $H_2I_2O_{10}^{4-}$ [14]. Nonetheless, for simplicity and consistency with previous reports, we refer to UV-illuminated periodate in this paper as UV/IO_4^-. Although highly effective, the Fenton and photo-Fenton processes were not investigated here because they require low pH [16], which is not suitable for alkaline wastewaters.

AOP performance was compared in terms of the initial rate of TOC removal and whether the treatment goal of 5 mg/L naphthenic acids could be reached. Because electrical energy can account for a significant fraction of AOP treatment costs [17], as well as the adverse environmental impacts associated with electricity generation, such as emissions of CO_2 and particulates, AOPs were also compared in terms of the electrical energy required to remove one half the TOC initial mass, and, for cases where the treatment goal was achieved, to lower the naphthenic acids concentration to 5 mg/L [17]. Because reactive species in the AOP systems are often pH dependent (e.g., H_2O_2 [18], the TiO_2 surface [19], and periodate [14]), and because oil sands process waters tend to be highly alkaline, the relative performance of the AOPs was evaluated at three alkaline pH values: pH 8 and 10, and in some cases pH 12. Finally, because the power requirements (and therefore operating costs) of a UV lamp are proportional in part to the wavelengths of light it emits, we evaluated the relative performance of the AOPs with Vycor and Pyrex filters surrounding a medium pressure Hg lamp to allow transmission of different regions of the UV spectrum, in order to model the performance of low pressure mercury (Hg) lamps (for the Vycor filter) as well as solar radiation (for the Pyrex filter). This setup allowed us to identify those components of the UV spectrum necessary for each AOP to degrade naphthenic acids, all using the same photochemical reactor. Use of a high power medium pressure Hg lamp versus a lower power low pressure Hg lamp also allowed us to complete a number of experiments in a reasonable time period.

2. Experimental

2.1. Chemical reagents

A commercial mixture of naphthenic acids ("naphthenic acids"), Ludox HS-30 colloidal silica (SiO_2), and *n*-butyl chloride were purchased from Sigma–Aldrich (St. Louis, MO). Sodium silicate ($Na_2SiO_3{\cdot}9H_2O$), sodium hydroxide (50 wt%), sodium chloride, and 30% H_2O_2 were obtained from Fisher Scientific (Fairlawn, NJ). Periodic acid (H_5IO_6) and sodium persulfate ($Na_2S_2O_8$) were from Acros, NJ. TiO_2 Aeroxide® P 25 was from Degussa (Akron, OH). The manufacturer-reported specific surface area of the TiO_2 was $50 \pm 15\ m^2/g$. Fresh nanopure water (18.1 MΩ cm) from an Infinity™ ultrapure water system (model D8961, Barnstead; Dubuque, IA) was used to prepare all solutions.

2.2. Photochemical experiments

Photochemical experiments were conducted in a reactor from Ace Glass (7841-06, Vineland, NJ) that was modified to fit a 16 mm diameter pH electrode. The reactor is illustrated in previous publications from the manufacturer [20] and our research [21]. The reactor was closed except for three small openings for inserting the pH electrode (Orion, 9802 BN), adding sodium hydroxide (NaOH), and sampling. It was held by a circular stand above a stir plate and magnetically stirred during experiments. The total solution volume was 1.3 L. The reactor contained a 450 W medium pressure Hg vapor lamp (Ace Glass model 7825-34) that was separated from the aqueous solution in which the photochemical reaction took place by a Quartz immersion well through which cooling water flowed continuously.

The radiated power (in W) from the lamp for each mercury emission line in the UV region was [20]: 366.0 nm: 25.6; 334.1 nm: 2.4; 313.0 nm: 13.2; 302.5 nm: 7.2; 296.7 nm: 4.3; 289.4 nm: 1.6; 280.4 nm: 2.4; 275.3 nm: 0.7; 270.0 nm: 1.0; 265.2 nm: 4.0; 257.1 nm: 1.5; 253.7 nm: 5.8; 248.2 nm: 2.3; 240.0 nm: 1.9; 238.0 nm: 2.3; 236.0 nm: 2.3; 232.0 nm: 1.5; 222.4 nm: 3.7. (There was also significant radiated power in the visible and IR regions; these data are available in a manufacturer publication [20], but are not reported here nor used in subsequent calculations). The total UV photon flux ($q_{p,TOT}$) in the photochemical reactor was calculated as follows from the UV radiated power values. First, the radiated power for each emission line was multiplied by 0.9 to account for 10% loss of power due to distance from the lamp surface to the inner wall of the immersion well, transmittance through the quartz wall of the immersion well, and through the cooling water contained in the immersion well [20]. This yielded values of radiated power at the immersion well outer surface (which is the inner surface of the aqueous phase reactor where the photochemical reaction took place) for each emission line. These values of power were then divided by the photon energy (i.e., hc/λ, where h is the Planck constant, c is the speed of light, and λ is the wavelength of the radiated energy) for that emission wavelength to yield values of photon flux (q_p) in units of photons/s. Summing the values of q_p for all UV emission lines yielded $q_{p,TOT}$, and summing the values in the UV A (400–320 nm), UV B (320–290 nm), and UV C (<290 nm) regions yielded values of the total UV photon flux in these wavelength regions, referred to hereafter for brevity as $q_{p,UV\,A}$, $q_{p,UV\,B}$, and $q_{p,UV\,C}$.

For selected experiments where noted, a Vycor or Pyrex filter sleeve (a tube open on both ends) (Ace Glass) was placed around the lamp to limit UV transmission to specific wavelengths. Values of $q_{p,TOT}$, $q_{p,UV\,A}$, $q_{p,UV\,B}$, and $q_{p,UV\,C}$ in the reactor when using these filters were calculated as described above, with the following additional adjustment: in addition to assuming 10% power loss through the Quartz immersion well and the cooling water that it contained, the radiated power was also multiplied by the fraction of UV radiation transmitted through the wall of the Vycor or Pyrex filter sleeve at each wavelength, using manufacturer reported values of transmittance versus wavelength [20].

Reagent concentrations were as follows: 100 mg/L naphthenic acids, 110 mg/L dissolved silicate (SiO_3^{2-}) (from 413 mg/L $Na_2SiO_3{\cdot}9H_2O$), 91 mg/L colloidal SiO_2, 1609 mg/L Na^+ (from 413 mg/L $Na_2SiO_3{\cdot}9H_2O$ and 3920 mg/L NaCl), and 2380 mg/L Cl^- (from 3920 mg/L NaCl). Naphthenic acids were added from a stock solution (1000 mg/L) prepared in 0.1 M NaOH. Solution pH was controlled at 8, 10, or 12 using a pH stat (Radiometer Analytical, Villeurbanne Cedex, France). All experimental conditions are listed in Table 1.

Samples were periodically taken from the reactor using a 30 mL plastic sterile Luer tip syringe that was attached to an 18-in. piece of Teflon tubing (i.d. 3 mm). Samples that contained TiO_2 were centrifuged at 10,000 rpm (relative centrifugal force: $4472 \times g$) for 30 min using a micro-centrifuge (Labnet International, Inc., USA). The supernatant was then analyzed for total organic carbon (TOC) using a Shimadzu TOC Analyzer (TOC 5050A/ASI 5000A). A five point standard curve was run daily, and standards and samples were analyzed using triplicate injections. The relative standard deviations of TOC concentrations based on triplicate injections

Table 1
Summary of experimental conditions and results.

Conditions	Filter[a]	pH	Initial rate (mg/L/min)[b]	Half-life (min)	$(EE/M)_{1/2}$ (kWh/kg TOC)[c]	Time to trt. goal (min)[d]	$(EE/M)_{trt.\,goal}$ (kWh/kg TOC)[e]	Chemical costs to meet trt. goal (USD/kg TOC)	Electricity costs to meet trt. goal (USD/kg TOC)
UV only	None	10		>360					
UV/TiO_2 (3 g/L)	None	8		>360					
UV/TiO_2 (3 g/L)	None	10		>360					
UV/IO_4^- (4 mM)	None	8	0.314 ± 0.057	>360					
UV/IO_4^- (4 mM)	None	10	0.32 ± 0.10	>360					
UV/IO_4^- (4 mM)	None	12	0.17 ± 0.10	>360					
UV/IO_4^- (10 mM)	None	10	0.63 ± 0.32	100	$(1.674 \pm 0.084) \times 10^4$				
UV/IO_4^- (20 mM)	None	10	0.48 ± 0.24	108	$(1.758 \pm 0.088) \times 10^4$				
UV/IO_4^- (50 mM)	None	10	0.52 ± 0.41	184	$(3.40 \pm 0.17) \times 10^4$				
UV/IO_4^- (10 mM)	Vycor	10	0.62 ± 0.49	128					
UV/IO_4^- (10 mM)	Pyrex	10		>360					
UV/$S_2O_8^{2-}$ (20 mM)	None	8	1.50 ± 0.41	18.6	$(3.67 \pm 0.18) \times 10^3$	38.6	$(4.05 \pm 0.22) \times 10^3$	82	401
UV/$S_2O_8^{2-}$ (20 mM)	None	10	2.0 ± 1.3	18.3	$(3.32 \pm 0.17) \times 10^3$	151	$(1.449 \pm 0.076) \times 10^4$	86	1440
UV/$S_2O_8^{2-}$ (1 mM)	None	10		>360					
UV/$S_2O_8^{2-}$ (10 mM)	None	10	1.20 ± 0.14	27.5	$(4.69 \pm 0.24) \times 10^3$				
UV/$S_2O_8^{2-}$ (20 mM)	Vycor	10	1.21 ± 0.22	27.8		87			
UV/$S_2O_8^{2-}$ (20 mM)	Pyrex	10	0.068 ± 0.026	340					
UV/H_2O_2 (50 mM)	None	8	1.62 ± 0.51	17.2	$(3.26 \pm 0.16) \times 10^3$	37	$(3.71 \pm 0.20) \times 10^3$	47	368
UV/H_2O_2 (50 mM)	None	10	0.87 ± 0.22	40	$(6.67 \pm 0.33) \times 10^3$				
UV/H_2O_2 (50 mM)	None	12	0.61 ± 0.26	62	$(1.040 \pm 0.052) \times 10^4$				
UV/H_2O_2 (1 mM)	None	10	0.1392 ± 0.0043	>360					
UV/H_2O_2 (4 mM)	None	10	0.30 ± 0.25	>360					
UV/H_2O_2 (10 mM)	None	10	0.95 ± 0.62	62	$(1.056 \pm 0.053) \times 10^4$				
UV/H_2O_2 (20 mM)	None	10	1.03 ± 0.40	31.3	$(5.55 \pm 0.28) \times 10^3$				
UV/H_2O_2 (50 mM)	Vycor	10	0.70 ± 0.13	102					
UV/H_2O_2 (50 mM)	Pyrex	10		>360					

[a] "None" means that only the Quartz immersion well was used.

[b] Uncertainties in initial rates are 95% confidence intervals. Initial rates are not reported when the 95% confidence interval included zero (i.e., when the slope of a plot of TOC concentration versus time was not significantly different from zero at the 95% confidence level).

[c] When the half life was not reached (i.e., half life > 360 min), values of $(EE/M)_{1/2}$ could not be calculated and are not shown. Uncertainties are one standard deviation determined by propagation of error.

[d] Values are given only when the treatment goal (3.4 mg/L TOC) was reached in approximately 6 h.

[e] Uncertainties are one standard deviation determined by propagation of error. When the treatment goal was not reached, values of $(EE/M)_{trt.\,goal}$ could not be calculated.

were typically less than 5%. Samples without TiO_2 were not centrifuged prior to TOC analysis. The initial concentration of TOC was approximately 67 mg/L, i.e., approximately 67% of the naphthenic acids mass consisted of carbon.

The concentration of *n*-butyl chloride was measured by headspace gas chromatography with flame ionization detection [22].

3. Results and discussion

3.1. Data handling

Initial rates (Table 1) were estimated by calculating the slopes of plots of TOC versus time by linear least squares regression using 4–6 data points taken during approximately the first 30–60 min of the reaction (during which time the slope was typically linear). Initial rates were calculated using the number of data points that yielded a slope with the largest coefficient of determination (R^2). Initial rates that were not statistically different from zero at the 95% confidence level are not reported.

The half life and the time required to reach the treatment goal (if it was reached) (Table 1) were estimated graphically from plots of TOC versus time using interpolation of smoothed lines connecting the data points. Considering that 67% of the naphthenic acids mass consisted of carbon (see above), a treatment goal of 5 mg/L naphthenic acids corresponds to 3.4 mg/L TOC. Values of the electrical energy per mass (EE/*M*) required to lower the TOC to one half its original value $(EE/M)_{1/2}$ and to achieve the treatment goal $(EE/M)_{trt.\,goal}$ (Table 1) were calculated using the approach in ref. [17], modified as in ref. [23]:

$$\left(\frac{EE}{M}\right)_{1/2} = \frac{Pt_{1/2}}{0.5[TOC]_0 V}\frac{(10^6\ mg/kg)}{60\ min/h} \quad (1)$$

$$\left(\frac{EE}{M}\right)_{trt.\,goal} = \frac{Pt_{trt.\,goal}}{V([TOC]_0 - 3.4\ mg/L)}\frac{(10^6\ mg/kg)}{60\ min/h} \quad (2)$$

where *P* is the lamp power consumption in kW, $t_{1/2}$ is the half life in minutes, $t_{trt.\,goal}$ is the time required to reach the treatment goal in minutes, *V* is the reactor volume in L, $[TOC]_0$ is the initial TOC concentration in mg/L (approximately 67 mg/L), and the remaining terms are conversion factors that yield values of EE/*M* in kWh $(kg\,TOC)^{-1}$. Because some of the lamp power was "wasted" when using the Vycor and Pyrex filters, $(EE/M)_{1/2}$ and $(EE/M)_{trt.\,goal}$ values for these conditions cannot be fairly compared to those calculated when no filter was used, and are not reported in Table 1. Values of the electrical energy required to remove a specific mass of TOC (EE/*M* values), and not values of the electrical energy to reduce the TOC concentration by an order of magnitude (electrical energy per order or EE/O values), are reported here since the experimental data conform to zero order or mixed kinetics (see figures), and not first order kinetics [17]. Since the initial TOC concentration was approximately 67 mg/L for all experimental conditions, values of $(EE/M)_{1/2}$ can be fairly compared even if zero order or mixed kinetics were observed.

3.2. Comparison of AOPs at pH 10

A series of experiments was performed at pH 10 to determine the concentrations of H_2O_2, periodate, and $S_2O_8^{2-}$ that resulted in the best removal of naphthenic acids (Fig. 1). Based on initial rates of TOC removal, $(EE/M)_{1/2}$ values, and whether the treatment goal of 3.4 mg/L TOC was reached, these concentrations were 10 mM for UV/IO_4^-, 20 mM for $UV/S_2O_8^{2-}$, and 50 mM for UV/H_2O_2 (Table 1, Fig. 1). The concentration of TiO_2 was not varied, but instead a concentration of 3 g/L was used for UV/TiO_2 experiments based on previous studies with the same experimental setup [21].

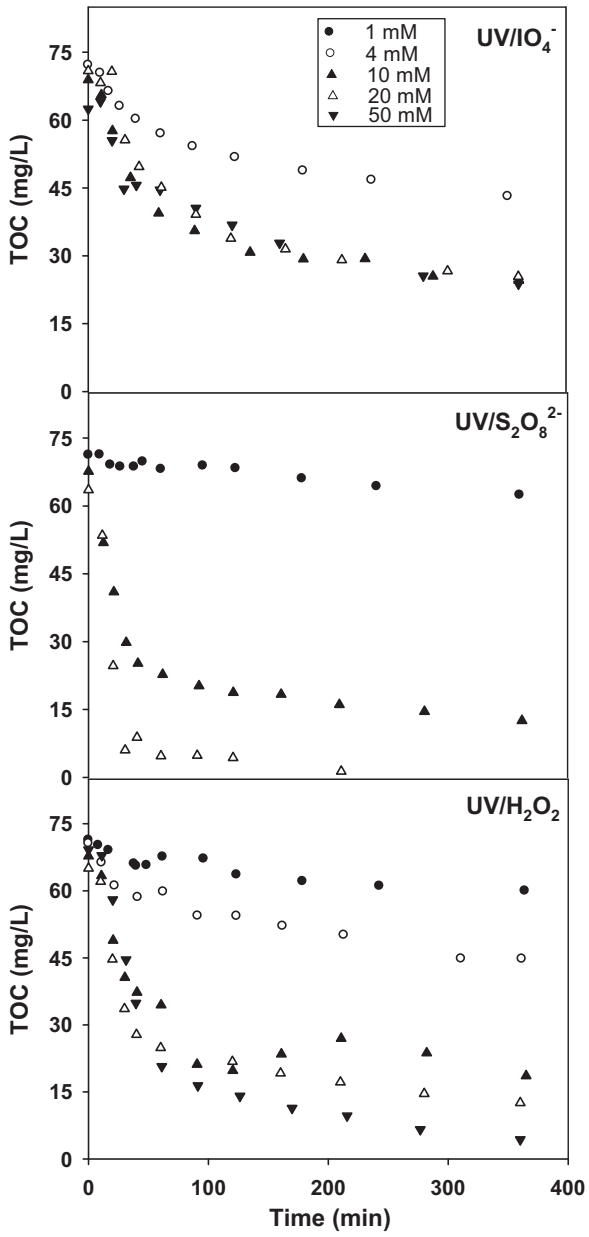

Fig. 1. Effect of reagent concentrations on transformation of naphthenic acids at pH 10 using the Quartz immersion well.

There was no significant degradation of naphthenic acids over approximately 6 h in the presence of these concentrations of periodate, $S_2O_8^{2-}$, H_2O_2, or TiO_2 at pH 10 when no UV light was used (data not shown), indicating that none of these reagents alone can directly oxidize naphthenic acids. Instead, radicals or other reactive species that form when aqueous solutions of periodate, $S_2O_8^{2-}$, H_2O_2, or TiO_2 are illuminated with UV light are responsible for naphthenic acids oxidation. Furthermore, when the UV lamp was turned on, but no TiO_2, H_2O_2, periodate, or $S_2O_8^{2-}$ were present in an aqueous solution adjusted to pH 10, there was limited (approximately 10%) transformation of naphthenic acids as TOC to total inorganic carbon (TIC) (i.e., bicarbonate and carbonate) over approximately 6 h (data not shown). McMartin et al. [24] also observed limited photolysis of naphthenic acids in the presence of UV light. As discussed below, most AOPs caused significantly faster oxidation of naphthenic acids than direct photolysis under their optimum conditions.

There was a general trend of increasing initial rates with increasing concentrations of periodate, $S_2O_8^{2-}$, and H_2O_2 (Table 1, Fig. 1), which can be explained by an increase in the steady state concentration of reactive radical species that are responsible for naphthenic acids oxidation. For UV/IO_4^-, however, a rate increase was observed when the periodate concentration increased from 4 to 10 mM, but not when the periodate concentration was increased further from 10 to 50 mM (Table 1, Fig. 1). Potentially reactive species generated in the UV/IO_4^- system include $IO_3^{\bullet}$, $HO^{\bullet}$, O_3, $IO_4^{\bullet}$, and $O(^3p)$ (oxygen atom) [14]. It is possible that reactions that consumed one or more of these reactive species, for example dimerization of $IO_3^{\bullet}$ or $IO_4^{\bullet}$ to form I_2O_6 or I_2O_8, respectively [14], counterbalanced any increase in steady state concentration of reactive species resulting from increased initial periodate concentrations, leading to reaction profiles that were essentially the same for 10, 20, and 50 mM periodate.

For UV/$S_2O_8^{2-}$, the treatment goal of 3.4 mg/L TOC was achieved for the optimum conditions (20 mM $S_2O_8^{2-}$) at pH 10 (Fig. 1, Table 1). For UV/H_2O_2 (50 mM H_2O_2), the TOC concentration was 4.3 mg/L after approximately 6 h at pH 10, which is close to the treatment goal. For UV/IO_4^-, however, TOC concentrations never approached the treatment goal at pH 10, despite varying the periodate concentration from 4 to 50 mM (Fig. 1). For UV/TiO_2, experiments at pH 10 did not show TOC removal significantly different from UV photolysis alone (data not shown).

Using the method of Liao et al. [25], we estimated the steady state concentration of $HO^{\bullet}$ in the UV/H_2O_2 system at pH 10 to be $(1.23 \pm 0.07) \times 10^{-12}$ M. The method of Liao et al. [25] involves measuring the pseudo first order rate constant for degradation of *n*-butyl chloride in the presence of $HO^{\bullet}$, then using the known second order rate constant for *n*-butyl chloride oxidation by $HO^{\bullet}$ to estimate the steady state concentration of $HO^{\bullet}$. This approach did not yield useful results for the UV/IO_4^- and UV/$S_2O_8^{2-}$ systems because *n*-butyl chloride reacted with periodate and $S_2O_8^{2-}$ even in the absence of UV light. We did not attempt to measure the steady state $HO^{\bullet}$ concentration in the UV/TiO_2 system due to potential confounding effects (e.g., involvement of other radicals or the TiO_2 surface) as well as the poor performance of UV/TiO_2 with respect to naphthenic acids degradation.

3.3. Effect of pH on AOP performance

Next, experiments were done to investigate the effect of pH on AOP performance. These experiments were done using the optimum concentrations of TiO_2, H_2O_2, or $S_2O_8^{2-}$. For UV/IO_4^-, however, preliminary experiments with 4 mM periodate indicated no effect of pH, and the results of the 4 mM experiments are reported here. Experiments with UV/TiO_2 and UV/$S_2O_8^{2-}$ were done at pH 8 and 10, and experiments with UV/IO_4^- and UV/H_2O_2 were done at pH 8, 10, and 12. For UV/TiO_2, experiments at 10 did not show naphthenic acids degradation significantly different from UV photolysis alone (data not shown). The poor performance of UV/TiO_2 for naphthenic acids oxidation compared to other substrates tested under similar conditions [21] may be due to electrostatic repulsion between the deprotonated naphthenic acids and the TiO_2 surface, which is negatively charged at pH 8 and 10 [19]. Due to its poor reactivity with the model wastewater at both pH 8 and 10, no further experiments were conducted with UV/TiO_2.

Concentration versus time profiles were nearly identical for naphthenic acids degradation by UV/IO_4^- (4 mM) at pH 8, 10, and 12 (Fig. 2), suggesting that the distribution of reactive species or their precursors were not pH dependent in the UV/IO_4^- system. It also suggests that the slowing of reaction rates as the reaction proceeded for UV/IO_4^- (Fig. 2) cannot be attributed to radical scavenging by CO_3^{2-} produced by TOC oxidation, since, for a given decrease in TOC and corresponding total inorganic carbon (TIC)

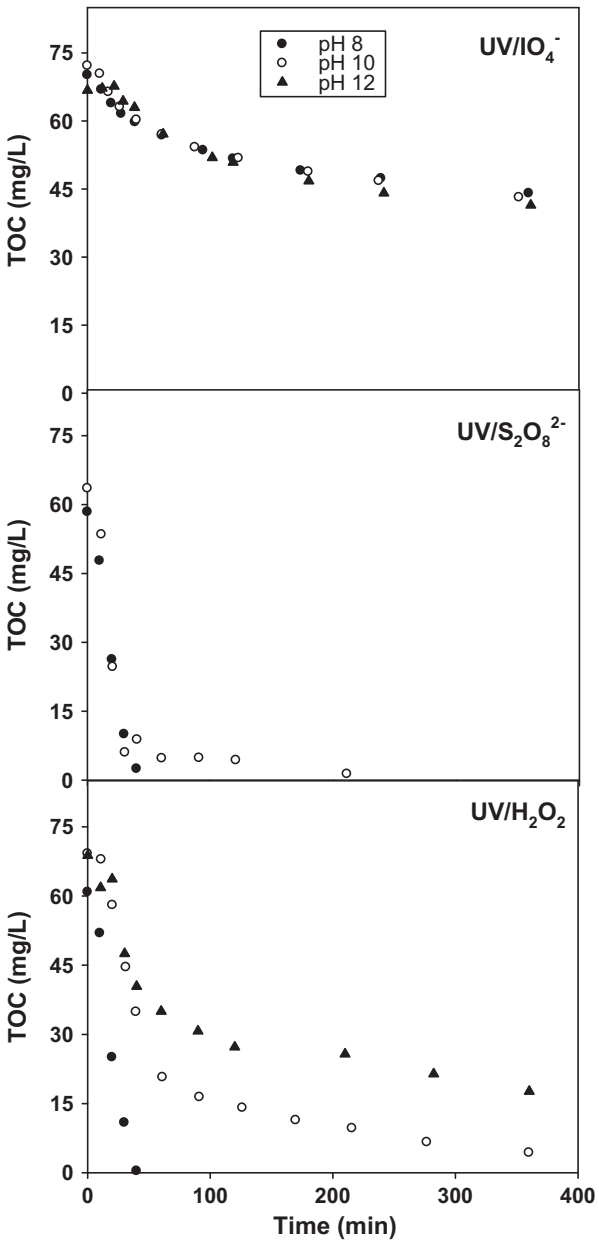

Fig. 2. Effect of pH on transformation of naphthenic acids using the Quartz immersion well. Reagent concentrations were 4 mM IO_4^-, 20 mM $S_2O_8^{2-}$, and 50 mM H_2O_2.

concentration, CO_3^{2-} would be present at significantly higher concentrations at pH 12, compared to pH 10, and at pH 10 compared to pH 8, yet the reaction profiles for naphthenic acids oxidation by UV/IO_4^- are nearly identical for all pH conditions. (The pK_a of HCO_3^- is 10.3.) It is possible that TOC removal slowed in the UV/IO_4^- system due to rapid oxidation of the most reactive components of the naphthenic acids mixture, leaving the more recalcitrant components behind. Other researchers have successfully modeled the kinetics of TOC degradation in photochemical systems assuming the existence of different TOC fractions that have different reactivities with radical species [26].

Experiments with UV/$S_2O_8^{2-}$ were performed at pH 8 and 10 only. It was not possible to raise and maintain the pH of the initial reaction solution for UV/$S_2O_8^{2-}$ at pH 12, perhaps because UV/$S_2O_8^{2-}$ causes a rapid pH drop due to reaction of sulfate radicals ($SO_4^{\bullet-}$), formed via photolysis of $S_2O_8^{2-}$, with water [27]:

$$SO_4^{\bullet-} + H_2O \rightarrow SO_4^{2-} + HO^{\bullet} + H^+ \quad (3)$$

While the reaction profiles for UV/$S_2O_8^{2-}$ were nearly identical at pH 8 and 10 for the first 30 min (Fig. 2), and the initial rates and $(EE/M)_{1/2}$ values are very similar for these two conditions (Table 1), it took almost four times longer to achieve the treatment goal of 3.4 mg/L at pH 10 compared to pH 8 (Table 1), meaning that the $(EE/M)_{trt.\,goal}$ value was also four times larger at pH 10 versus pH 8 (Eq. (2)). Specifically, the reaction for UV/$S_2O_8^{2-}$ at pH 8 went to completion very rapidly, with nearly zero order kinetics, while the reaction at pH 10 followed the same pattern until approximately 30 min, after which it slowed significantly (Fig. 2). The reaction rate may have slowed at pH 10 due to consumption of reactive species by CO_3^{2-}, i.e.,

$$CO_3^{2-} + R^{\bullet} \rightarrow CO_3^{\bullet-} + R^- \quad (4)$$

where $R^{\bullet}$ is a reactive radical species such as $HO^{\bullet}$ or $SO_4^{\bullet-}$. CO_3^{2-} can consume both sulfate ($SO_4^{\bullet-}$) and hydroxyl ($HO^{\bullet}$) radicals [28]. The lack of a statistically significant difference in initial rates or half lives for UV/$S_2O_8^{2-}$ (20 mM) at pH 8 and 10 (Table 1) is consistent with this explanation, since there would not yet have been significant accumulation of TIC (HCO_3^- and CO_3^{2-}) during the initial reaction period before significant TOC depletion. (Plots of TIC would mirror those of TOC).

Solution pH had the strongest influence on the transformation of naphthenic acids by UV/H_2O_2 (Fig. 2), with initial rates significantly lower and values of $(EE/M)_{1/2}$ significantly higher with increasing pH (Table 1). While the treatment goal of 3.4 mg/L TOC was only achieved for UV/H_2O_2 at pH 8, the TOC concentration after approximately 6 h for UV/H_2O_2 at pH 10 was close to the treatment goal (4.3 mg/L). To reach this concentration, however, took nearly ten times longer at pH 10 than at pH 8 (Fig. 2), with a corresponding 10-fold increase in required electricity (Eq. (2)).

The principle of UV/H_2O_2 is photolysis of H_2O_2 [29]:

$$H_2O_2 + h\nu \rightarrow 2HO \quad (5)$$

which takes place below the pK_a of H_2O_2 (11.6 [18]). The pH dependence of H_2O_2 speciation can explain the differences in reactivity in the UV/H_2O_2 system at pH 10 and 12, but not between pH 8 and 10, since the concentration of undissociated H_2O_2 would be nearly identical at pH 8 and 10. Neither can scavenging of $HO^{\bullet}$ by CO_3^{2-} produced by TOC oxidation entirely explain the decreased performance of UV/H_2O_2 with increasing pH, since initial reaction rates for UV/H_2O_2 (50 mM) decrease steadily from pH 8 to 12 (Table 1), yet significant accumulation of CO_3^{2-} would not have occurred during the initial reaction period from which initial rates were calculated. Self decomposition of H_2O_2:

$$2H_2O_2 \rightarrow 2H_2O + O_2 \quad (6)$$

which proceeds rapidly at alkaline pH [30] could have contributed to the relatively poor performance of UV/H_2O_2 at higher pH values.

3.4. Effect of UV wavelength

Finally, experiments at the optimum concentrations of periodate, $S_2O_8^{2-}$, or H_2O_2 were repeated at pH 10 using Vycor and Pyrex filters around the Quartz immersion well in order to compare the efficiency of UV/IO_4^-, UV/$S_2O_8^{2-}$, and UV/H_2O_2 under conditions simulating the use of low pressure Hg lamps for the Vycor filter, or solar radiation for the Pyrex filter (Fig. 3). Fig. 4 shows the calculated q_p entering the reactor for each of the emission lines of the Hg lamp in the UV region, and for each of the relevant conditions, i.e., with no filter, with the Vycor filter, and with the Pyrex filter. Calculated values of $q_{p,TOT}$ as well as $q_{p,UV\,A}$, $q_{p,UV\,B}$, and $q_{p,UV\,C}$ entering the reactor for the Quartz immersion well only, and with the Vycor and Pyrex sleeves, are illustrated in Fig. 5. The Hg emission line at 253.7 nm was included neither in Figs. 4 and 5 nor in the related calculations, since the corresponding energy is absorbed or reflected inward by the quartz surrounding the lamp [20]. Fig. 5 shows that $q_{p,UV\,A}$ did not vary significantly among the experimental setups (because neither Quartz, Vycor, nor Pyrex blocks UV A to a significant extent), and that the decline in $q_{p,TOT}$ when using the Vycor and Pyrex filters was due primarily to a decrease in $q_{p,UV\,B}$ and $q_{p,UV\,C}$.

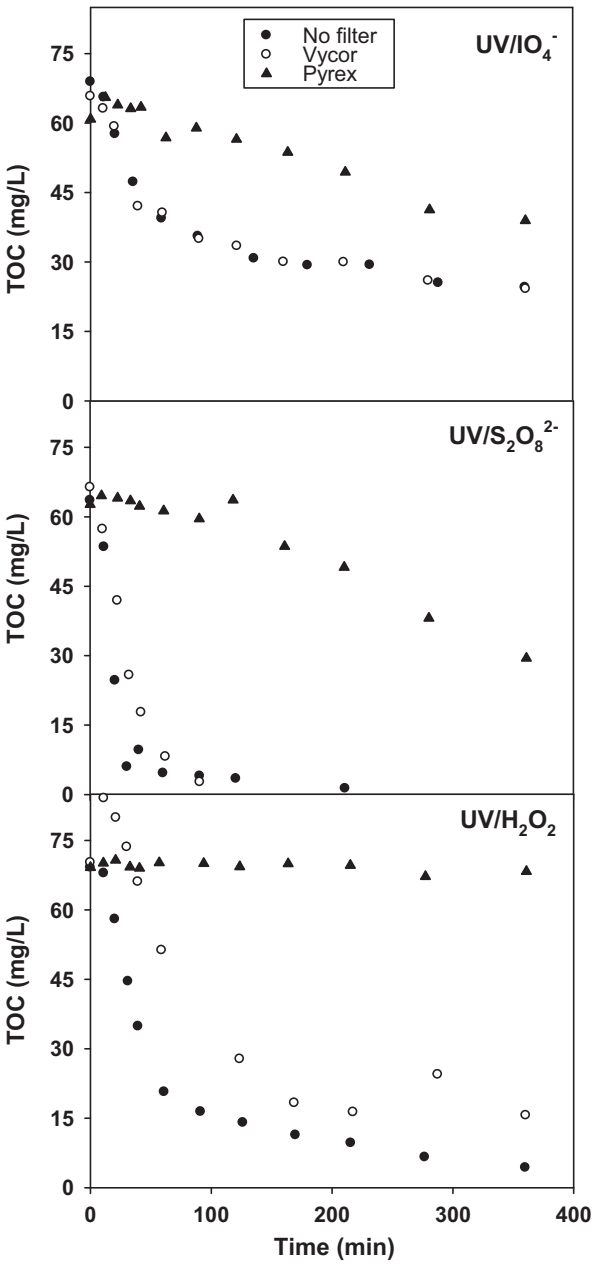

Fig. 3. Effect of UV filters on the transformation of naphthenic acids at pH 10. "No filter" means only the Quartz immersion well was used. Reagent concentrations were 10 mM IO_4^-, 20 mM $S_2O_8^{2-}$, and 50 mM H_2O_2.

For UV/IO_4^-, there was no significant difference in reaction profiles (Fig. 3) for the Quartz versus the Vycor filters. The Pyrex filter significantly slowed the reaction, however, and unlike when only the Quartz immersion well or the Vycor filter were used, the reaction did not reach the half life in 6 h when the Pyrex filter was used (Fig. 3, Table 1). The peak UV absorbance for periodate is between 200 and 250 nm, with some absorbance at wavelengths up to approximately 310 nm [31]. The difference in wavelengths transmitted by the Vycor and Pyrex filters (Section 2.2), specifically

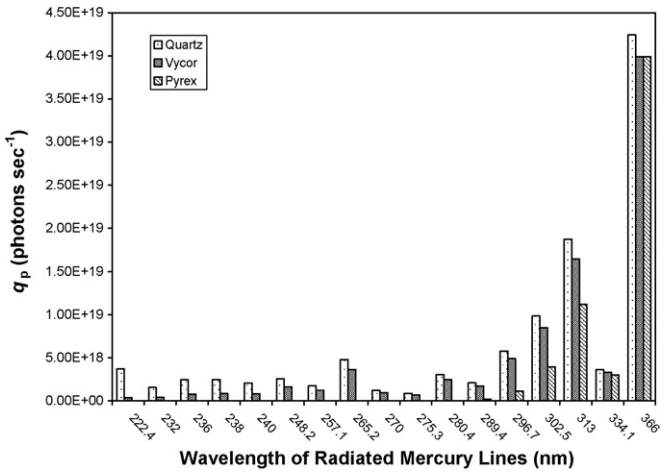

Fig. 4. Photon flux for the UV region of the medium pressure Hg lamp.

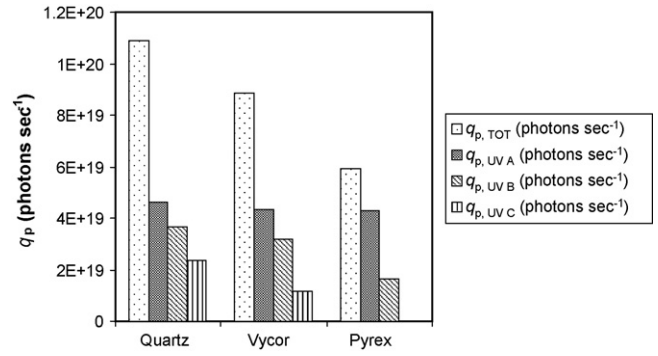

Fig. 5. Photon flux for the Quartz immersion well only, and for the Vycor and Pyrex filters. (UV A = 400–320 nm; UV B = 320–290 nm; UV C < 290 nm.)

the complete elimination of high energy UV C radiation when the Pyrex filter was used (Fig. 5), can explain the difference in reactivity of UV/IO_4^- with naphthenic acids when using these filters.

For UV/$S_2O_8^{2-}$, the reaction profiles (Fig. 3) were also similar for Quartz and Vycor, but much poorer for Pyrex. Similar to UV/IO_4^-, this is consistent with the UV absorption spectrum of $S_2O_8^{2-}$; specifically, a peak UV absorbance at <250 (a wavelength region completely eliminated when using the Pyrex filter (Fig. 5)), with some absorbance between 300 and 350 nm [15].

UV/$S_2O_8^{2-}$ was the only AOP system for which the treatment goal was achieved using the Vycor filter (Table 1), meaning that this system could potentially be used for naphthenic acids degradation using low pressure Hg lamps that emit light primarily around 254 nm, and that have lower rates of electricity use (power) than medium pressure Hg lamps that emit light with higher energy wavelengths. While the reaction profiles for the Quartz (no filter) and Vycor filter are very similar for the first 30–60 min in the UV/$S_2O_8^{2-}$ system (Fig. 3), it took nearly twice as long to reach the treatment goal when using only the Quartz immersion well (no filter) compared to the Vycor filter (Table 1). There is no obvious explanation for this finding, except the possible generation of a species that short circuits a radical chain reaction in the absence of the Vycor filter.

For UV/H_2O_2, there was a significant difference in the reaction profiles (Fig. 3) for the Quartz and Vycor filters, and an essentially complete inhibition of the reaction when the Pyrex filter was used (Fig. 3). While wavelengths less than 365 nm are sufficient to cause photolysis of H_2O_2 to HO• [29], the molar absorptivity of H_2O_2 is greater at lower wavelengths, with extremely low absorption and insignificant photolysis of H_2O_2 at wavelengths of 350 nm and above [32]. Thus, the higher energy wavelengths transmitted by the Quartz immersion well and the Vycor filter in the UV C region (Fig. 5) are needed to generate a steady state concentration of HO• sufficient to transform naphthenic acids in a reasonable time period.

Values of initial rate of TOC removal (Table 1) were plotted versus $q_{p,TOT}$ for UV/H_2O_2 (50 mM) and UV/$S_2O_8^{2-}$ (20 mM) at pH 10 (not shown). The initial rate for UV/H_2O_2 with the Pyrex filter was set equal to zero for this purpose based on the near constant concentration of TOC over 6 h for these conditions (Fig. 3). While there was some TOC removal for the UV/IO_4^- system with the Pyrex filter (Fig. 3) the data did not yield an initial rate significantly different from zero at the 95% confidence level, so a plot of initial rate versus $q_{p,TOT}$ was not prepared since it would have contained only two data points. Consistent with the expected relationship between photon flux and reactivity, there were reasonable correlations between initial rate and $q_{p,TOT}$ for the UV/$S_2O_8^{2-}$ (20 mM) and UV/H_2O_2 (50 mM) systems at pH 10, with the following linear regression equations: (1) for UV/$S_2O_8^{2-}$, Initial rate = $(-2.245 \pm 0.034) + (3.89 \pm 0.038) \times 10^{-20} \times q_{p\,TOT}$ ($R^2 = 1.00$), and (2) for UV/H_2O_2, Initial rate = $(-1.0 \pm 4.8) + (1.8 \pm 5.4) \times 10^{-20} \times q_{p\,TOT}$ ($R^2 = 0.95$). (In both equations, the initial rate has units of mg/L/min and $q_{p,TOT}$ has units of photons/s). The slope of the linear regression for the UV/H_2O_2 system is not significantly different from zero at the 95% confidence level, which likely results from both imperfect correlation and only three data points (i.e., data obtained for the Quartz, Vycor, and Pyrex systems).

Initial rates were also fairly well correlated with values of $q_{p,UV\,A}$, $q_{p,UV\,B}$, and $q_{p,UV\,C}$ (not shown), which can be explained by the fact that the decrease in $q_{p,TOT}$ upon using the Vycor and Pyrex filters was due to decreases in fluxes in all regions of the UV spectrum (even $q_{p,UV\,A}$ decreased slightly upon using the Vycor and Pyrex filters—see Fig. 5). The majority of the decrease in $q_{p,TOT}$ when using the Vycor and Pyrex filters, however, was due to decreases in $q_{p,UV\,B}$ and $q_{p,UV\,C}$ (Fig. 5). Thus, consistent with the earlier discussion in this section, the decrease in initial rates and/or complete stop in reactivity when using the Vycor and Pyrex filters at pH 10 for UV/H_2O_2 (50 mM) and UV/$S_2O_8^{2-}$ (20 mM) can be explained by the attenuation of high energy wavelengths in the UV B and C regions. Photons with these wavelengths are essential for naphthenic acids degradation by UV/H_2O_2 and UV/$S_2O_8^{2-}$, and these AOPs will not be effective with solar radiation.

4. Conclusions

The treatment goal of 3.4 mg/L TOC (approximately 5 mg/L naphthenic acids) was achieved under four conditions, including UV/$S_2O_8^{2-}$ (20 mM) at pH 8 and 10, and UV/H_2O_2 (50 mM) at pH 8 (all with the Quartz immersion well). The amount of electricity required to reach the treatment goal (reflected in the $(EE/M)_{trt,goal}$ values), as well as the adverse environmental impacts associated with generation of this electricity, were about equal for UV/$S_2O_8^{2-}$ (20 mM) and UV/H_2O_2 (50 mM) at pH 8 (Table 1). Electricity requirements for treatment by UV/$S_2O_8^{2-}$ (20 mM) at pH 10 were three to four times larger, indicating better performance of UV/$S_2O_8^{2-}$ at pH 8 versus pH 10, possibly due to greater scavenging of $SO_4^{\bullet-}$ or HO• by CO_3^{2-} at pH 10. For UV/$S_2O_8^{2-}$ and UV/H_2O_2 at pH 10, initial rates were correlated fairly well with total $q_{p,TOT}$, and photons in the UV B and UV C regions were necessary for the reaction to occur to a significant extent.

Treatment by UV/$S_2O_8^{2-}$ has the disadvantages of producing treated water that contains significant residual sulfate [15], while the decomposition of H_2O_2 yields only water and oxygen (reaction (6)). UV light increases the rate of H_2O_2 decomposition [33], so residual H_2O_2 would potentially degrade quickly in a setting

exposed to sunlight, such as an outdoor treatment pond. The electricity and chemical costs, in units of U.S. dollars (USD) per kg of TOC removed, estimated by extrapolation of data from our 1.3 L bench scale reactor, are given in Table 1 for the three conditions described above. Electricity costs were estimated using data from the U.S. Department of Energy, Energy Information Administration [34] and chemical costs were estimated using online market sources [35]. In addition to chemical and electricity costs and post-treatment water quality requirements, the environmental impacts of production of treatment chemicals (e.g., H_2O_2, $S_2O_8^{2-}$ salts, and NaOH or other caustic reagents) should also be considered in choosing a treatment option, preferably using life cycle assessment.

Use of UV/$S_2O_8^{2-}$ (20 mM) at pH 10 with the Vycor filter covering the Quartz immersion well also achieved the treatment goal. Because some of the power associated with the medium pressure Hg lamp was "wasted" by blocking high energy radiation with the Vycor filter, the $(EE/M)_{trt.\,goal}$ value for this condition cannot be fairly compared with those for the other conditions that met the treatment goal (all of which used the Quartz immersion well), and thus is not reported in Table 1. But the fact that UV/$S_2O_8^{2-}$ met the treatment goal using a Vycor filter indicates that treatment of naphthenic acids by UV/$S_2O_8^{2-}$ with low pressure Hg lamps that consume less electricity may be feasible. The poor performance of UV/IO_4^-, UV/$S_2O_8^{2-}$, and UV/H_2O_2 when the Pyrex filter was used (Fig. 3) indicates that use of solar radiation for naphthenic acids removal using these AOPs is not feasible, at least under the conditions tested here.

Good naphthenic acids removal was achieved under several conditions despite a very high ionic strength and the presence of colloidal silica, although these conditions likely contributed to the poor performance of UV/TiO_2. While chloride can react with $HO^\bullet$ and $SO_4^{\bullet-}$ (producing unreactive OH^- and SO_4^{2-}) [27], if such radical scavenging reactions occurred to a significant extent in these experiments, they did not interfere with reaching the treatment goal in a reasonable period.

The $(EE/M)_{1/2}$ values for the AOP conditions where the treatment goal was reached are similar in magnitude to those reported for photochemical transformation of dichloroacetic acid by UV/TiO_2 and UV/H_2O_2 using a variety of UV lamps and reactor configurations [23]. Bolton et al. [17] have shown, through consideration of photochemical and reactor efficiencies, that the minimum possible EE/M for oxidation of a hypothetical contaminant with a molecular weight of 100 g/mol using a photochemical AOP is 87.2 kWh $(kg\,TOC)^{-1}$. This low value assumes many ideal conditions (unlikely to be achieved in real treatment systems), including that only two reactive radicals are required to oxidize each carbon atom, a quantum yield of 1 (100%) for formation of such radicals, and that 25% of the lamp power consumed yields useful photons with an average energy of 254 nm. As a practical matter, improvement of (i.e., lowering) the $(EE/M)_{trt.\,goal}$ values for treatment of naphthenic acids will require choosing UV lamps with emission spectra tailored to the required wavelength for that AOP—information reported in this study. To illustrate, Li et al. [36] concluded that the total electricity required for treatment of alcohols would be five times higher using a smaller number of medium pressure (broad spectrum) versus a larger number of low pressure (narrow spectrum) Hg lamps due to the unutilized wavelengths in the medium pressure lamps.

Acknowledgements

Financial support for this research was provided by ConocoPhillips. We thank Rebecca Long for help with many experiments, and the reviewers for critical evaluation of the manuscript.

References

[1] E.W. Allen, Process water treatment in Canada's oil sands industry: I. Target pollutants and treatment objectives, J. Environ. Eng. Sci. 7 (2008) 123–138.
[2] F.M. Holowenko, M.D. MacKinnon, P.M. Fedorak, Characterization of naphthenic acids in oil sands wastewaters by gas chromatography-mass spectrometry, Water Res. 36 (2002) 2843–2855.
[3] J.V. Headley, D.W. McMartin, A review of the occurrence and fate of naphthenic acids in aquatic environments, J. Environ. Sci. Health A Tox. Hazard. Subst. Environ. Eng. 39 (2004) 1989–2010.
[4] D.M. Petković, M.S. Ristić, The dipole-moment, self association and dissociation of naphthenic acid, J. Serb. Chem. Soc. 52 (1987) 641–647.
[5] E.W. Allen, Process water treatment in Canada's oil sands industry: II. A review of emerging technologies, J. Environ. Eng. Sci. 7 (2008) 499–524.
[6] N. Fong, S. Ng, K.H. Chung, Y. Tu, Z. Li, B.D. Sparks, L.S. Kotlyar, Bitumen recovery from model systems using a warm slurry extraction process: effects of oilsands components and process water chemistry, Fuel 83 (2004) 1865–1880.
[7] M.D. MacKinnon, H. Boerger, Description of two treatment methods for detoxifying oil sands tailings pond water, Water Pol. Res. J. Canada 21 (1986) 496–512.
[8] S.A. Thomas, M.E. Yost, S.R. Cathey, Silica removal from steam-flood produced water: South Texas tar sands pilot, SPE Prod. Eng. 2 (1987) 131–136.
[9] A.C. Scott, W. Zubot, M.D. MacKinnon, D.W. Smith, P.M. Fedorak, Ozonation of oil sand process water removes naphthenic acids and toxicity, Chemosphere 71 (2008) 156–160.
[10] G.V. Buxton, C.L. Greenstock, W.P. Helman, A.B. Ross, Critical review of rate constants for reactions of hydrated electrons, hydrogen atoms, and hydroxyl radicals ($^\bullet OH/^\bullet O^-$) in aqueous solution, J. Phys. Chem. Ref. Data 17 (1988) 513–886.
[11] S. Chen, G. Cao, Photocatalytic oxidation of nitrite by sunlight using TiO_2 supported on hollow glass microbeads, Sol. Energy 73 (2002) 15–21.
[12] R.J. Brandi, O.M. Alfano, A.E. Cassano, Evaluation of radiation absorption in slurry photocatalytic reactors. 1. Assessment of methods in use and new proposal, Environ. Sci. Technol. 34 (2000) 2623–2630.
[13] T. Oppenlander, Photochemical Purification of Water and Air, Wiley-VCH, Weinheim, Germany, 2003.
[14] L.K. Weavers, I. Hua, M.R. Hoffmann, Degradation of triethanolamine and chemical oxygen demand reduction in wastewater by photoactivated periodate, Water Environ. Res. 69 (1997) 1112–1119.
[15] H. Hori, A. Yamamoto, E. Hayakawa, S. Taniyasu, N. Yamashita, S. Kutsuna, Efficient decomposition of environmentally persistent perfluorocarboxylic acids by use of persulfate as a photochemical oxidant, Environ. Sci. Technol. 39 (2005) 2383–2388.
[16] J.M. Poyatos, M.M. Muñio, M.C. Almecija, J.C. Torres, E. Hontoria, F. Osorio, Advanced oxidation processes for wastewater treatment: state of the art, Water Air Soil Pollut. 205 (2010) 187–204.
[17] J.R. Bolton, K.G. Bircher, W. Tumas, C.A. Tolman, Figures-of-merit for the technical development and application of advanced oxidation technologies for both electric- and solar-driven systems, Pure Appl. Chem. 73 (2001) 627–637.
[18] J. Staehelin, J. Hoigné, Decomposition of ozone in water: rate of initiation by hydroxide ions and hydrogen peroxide, Environ. Sci. Technol. 16 (1982) 676–681.
[19] M. Kosmulski, pH-dependent surface charging and points of zero charge II. Update, J. Colloid Interface Sci. 275 (2004) 214–224.
[20] Ace Glass, Product Manual 7825—Spectral Energy Distribution, Ace Glass, Vineland, NJ, 2008 (accessed February 18, 2011) http://www.aceglass.com/dpro/kb_article.php?ref=2881-QRTB-2268.
[21] X. Zhu, S.R. Castleberry, M.A. Nanny, E.C. Butler, Effect of pH and catalyst concentration on photocatalytic oxidation of aqueous ammonia and nitrite in titanium dioxide suspensions, Environ. Sci. Technol. 39 (2005) 3784–3791.
[22] X. Zhu, M.A. Nanny, E.C. Butler, Photocatalytic oxidation of aqueous ammonia in model gray waters, Water Res. 42 (2008) 2736–2744.
[23] C.S. Zalazar, M.L. Satuf, O.M. Alfano, A.E. Cassano, Comparison of H_2O_2/UV and heterogeneous photocatalytic processes for the degradation of dichloroacetic acid in water, Environ. Sci. Technol. 42 (2008) 6198–6204.
[24] D.W. McMartin, J.V. Headly, D.A. Friesen, K.M. Peru, J.A. Gillies, Photolysis of naphthenic acids in natural surface water, J. Environ. Sci. Health A Tox. Hazard. Subst. Environ. Eng. 39 (2004) 1361–1383.
[25] C. Liao, S. Kang, F. Wu, Hydroxyl radical scavenging role of chloride and bicarbonate ions in the H_2O_2/UV process, Chemosphere 44 (2001) 1193–1200.
[26] F.J. Beltrán, A. Aguinaco, J.F. García-Araya, Kinetic modeling of TOC removal in the photocatalytic ozonation of diclofenac aqueous solutions, Appl. Catal. B: Environ. 100 (2010) 289–298.
[27] X. Yu, Z. Bao, J.R. Barker, Free radical reactions involving $Cl^\bullet$, $Cl_2^{\bullet-}$, and $SO_4^{\bullet-}$ in the 248 nm photolysis of aqueous solutions containing $S_2O_8^{2-}$ and Cl^-, J. Phys. Chem. A 108 (2004) 295–308.
[28] D.M. Stanbury, Reduction potentials involving inorganic free radicals in aqueous solution, in: A.G. Sykes (Ed.), Advances in Inorganic Chemistry, vol. 33, Academic Press, San Diego, 1989, p. 109.
[29] J.H. Baxendale, J.A. Wilson, The photolysis of hydrogen peroxide at high light intensities, Trans. Faraday Soc. 53 (1957) 344–356.
[30] W. Chu, Modeling the quantum yields of herbicide 2,4-D decay in UV/H_2O_2 process, Chemosphere 44 (2001) 935–941.

[31] S. Irmak, E. Kusvuran, O. Erbatur, Degradation of 4-chloro-2-methylphenol in aqueous solution by UV irradiation in the presence of titanium dioxide, Appl. Catal. B 54 (2004) 85–91.
[32] C.C. Wong, W. Chu, The hydrogen peroxide-assisted photocatalytic degradation of alachlor in TiO_2 suspensions, Environ. Sci. Technol. 37 (2003) 2310–2316.
[33] M. Qureshi, M.K. Rahman, Photolysis of aqueous solutions of hydrogen peroxide, J. Phys. Chem. 36 (1932) 664–669.
[34] U.S.Department of Energy, Energy Information Administration, Average Retail Price of Electricity to Ultimate Customers by End-Use Sector, by State, U.S. Department of Energy, Washington, DC, 2011 (accessed February 25, 2011) http://www.eia.doe.gov/cneaf/electricity/epm/table5_6_b.html.
[35] http://www.alibaba.com (accessed February 25, 2011) and http://www.dhgate.com (accessed February 25, 2011).
[36] K. Li, D.R. Hokanson, J.C. Crittenden, R.R. Trussell, D. Minakata, Evaluating UV/H_2O_2 processes for methyl tert-butyl ether and tertiary butyl alcohol removal: effect of pretreatment options and light sources, Water Res. 42 (2008) 5045–5053.